

# Sequence-Selective Metal Ion Binding to DNA Hexamers

Signe Steinkopf and Einar Sletten\*

Department of Chemistry, University of Bergen, Allegt. 41, N-5007 Bergen, Norway

Steinkopf, S. and Sletten, E., 1994. Sequence-Selective Metal Ion Binding to DNA Hexamers. – Acta Chem. Scand. 48: 388–392 © Acta Chemica Scandinavica 1994.

Base-selective interaction between divalent metal ions and DNA oligomers has been studied by 1D and 2D NMR spectroscopy. Titration with paramagnetic metal ions induces selective line broadening of resonances from protons close to the binding site. Also the intensities of 2D NOESY cross-peaks involving paramagnetic affected protons will be quenched. Two hexamers, 5'-d(CGTACG)<sub>2</sub> (**I**) and 5'(GCATGC)<sub>2</sub> (**II**) have been titrated with Mn(II) ions. Manganese binds selectively to the terminal guanine, G1, in sequence **II** as manifested through pronounced paramagnetic line broadening and loss of intensities of NOESY cross-peaks involving G-H8 protons. The second guanine, G5, and the non-guanine residues are appreciably less affected. In sequence **I** both guanines, G2 and G6, are the targets for selective metal binding as judged from G-H8 line broadening. The extent of interaction is almost identical for the two G-residues and comparable to that observed for G1 in sequence **II**. The metal binding site in the duplexes is most likely nitrogen G-N7. Selective metal binding to oligonucleotides may be related to sequence-dependent variation in molecular electrostatic potentials (MEP) along the chain.

The interaction of metal ions with DNA is an active area of research, particularly in the development of new anti-tumor drugs.<sup>1</sup> Platinum anti-cancer drugs have been reported to interact with guanine residues in DNA.

Platination of DNA from salmon sperm followed by enzymatic degradation and chromatographic analysis showed a predominance of Pt-GpG species (65%), a somewhat smaller portion of Pt-ApG (25%) but no Pt-GpA.<sup>2</sup> Studies of interaction between Ca(II)<sup>3,4</sup> or Mg(II)<sup>5</sup> with DNA indicate site-specific metal binding. Over the past few years we have studied metal ion interaction with different DNA oligonucleotide sequences. The first results from these type of investigations<sup>6</sup> indicated that Zn(II) and Mn(II) ions bind selectively to the oligonucleotide d(CGCGAATTCGCG)<sub>2</sub>. The guanines were found to be the predominant binding sites, in agreement with earlier metal-DNA studies. However, for the first time a remarkable sequence-selective metal binding pattern was revealed in which the guanine bases were affected in the order G4 ≫ G2, G10 and G12.

In a recent <sup>1</sup>H NMR chemical shift study of the interaction between Zn(II) ions and the double helix 5'-ATGGGTACCCAT differential Zn binding was found.<sup>7</sup> Further work by Frøystein *et al.*<sup>8</sup> on manganese interaction with a series of ten different oligonucleotides showed that metal ions bind selectively to guanine residues on the 5'-side in the following order: 5'-GG > 5'-GA > 5'-

GT > 5'-GC. No clear evidence of binding to 5'-G in 5'-GC steps or to non-G residues was found. Recently Frøystein and Sletten<sup>9</sup> have monitored titration experiments of Hg(II) ions to the DNA dodecamer duplex 5'-d(CGCGAATTCGCG)<sub>2</sub> by <sup>1</sup>H and <sup>15</sup>N NMR spectroscopy, and found that Hg(II) interacts selectively with the AT-tract of the oligomer.

Theoretical calculations of the molecular electrostatic potentials (MEPs) along the double helix show marked sequence-dependent variations.<sup>10</sup> Fluctuation in the nucleophilicity of G-N7 sites as a consequence of subtle sequence-dependent conformational changes that alter base stacking could account for the metal binding pattern. Alkylation reactions in which positively charged groups attack specific G-residues at N7, producing a six- to eight-fold variation in methylation activity in DNA fragments, strongly support the idea of sequence-dependent variation in N7 nucleophilicity.<sup>11</sup>

In order to probe further the rules of sequence-selective metal binding to DNA we present here results of titration experiments involving two DNA 5'-3' inverted hexamers, 5'-d(CGTACG)<sub>2</sub> (**I**) and 5'-d(GCATGC)<sub>2</sub> (**II**). Sequence **II** comprises the specific target site for the restriction endonuclease *Sph*I. In a comparison of metal ion affinity between **I** and **II** we are able to observe terminal 3'-residues vs. 5'-residues and GT base step vs. GC step. The interactions between these oligomers and MnCl<sub>2</sub> have been monitored by observing <sup>1</sup>H NMR paramagnetic line-broadening and loss of 2D NOESY

\* To whom correspondence should be addressed.

cross-peak intensities. The line-broadening effects are assumed to be dominated by scalar paramagnetic relaxation, which in turn rules out the possibility of obtaining precise geometric information.<sup>12</sup> Nevertheless, the method is a quite powerful tool for pinpointing possible binding sites in a qualitative manner.<sup>13</sup>

## Experimental

The DNA hexamers 5'-(CGTACG) (**I**) and 5'-(GCATGC) (**II**) were synthesized by using solid-phase phosphite triester techniques as previously described.<sup>14</sup> The synthetic DNA samples were purified by chromatography in distilled water on a 120 cm Sephadex G-25 column and lyophilized to dryness. The sequences were palindromes which readily form duplexes. The lyophilized samples were dissolved in 0.4 ml solution containing 0.15 mM EDTA and 20 mM sodium phosphate adjusted to pH 7.0 with NaOH. EDTA was added to prevent effects from paramagnetic impurities. The DNA samples were lyophilized to dryness from D<sub>2</sub>O and redissolved in 99.96% D<sub>2</sub>O. Finally the samples were dissolved in 0.4 ml of 99.996% D<sub>2</sub>O and transferred to 5 mm NMR tubes. Each sample contained approximately 400 OD<sub>260</sub> units, corresponding to ca. 4.8 mM in duplex oligomer. A stock solution of 0.02 M MnCl<sub>2</sub> made up in D<sub>2</sub>O was lyophilized to dryness and redissolved in 99.96% D<sub>2</sub>O. The final concentration of MnCl<sub>2</sub> was 0.52 mM after dilution in D<sub>2</sub>O.

All spectra were recorded on a Bruker AM-400 MHz wide-bore spectrometer at 400.13 MHz. The temperature was 303 K in all experiments. One-dimensional spectra were typically recorded into 4096 complex point with a 3479 spectral width. The spectra were obtained after 128 transients with pulse width 8.5 ms and recycling delay of 5 s. COSY and NOESY experiments were used to confirm previous proton assignments of the hexamers.<sup>15,16</sup> NOESY experiments were also used to examine the effects of paramagnetic ion interaction on the cross-peak intensities. COSY and NOESY spectra were collected in phase-sensitive mode with quadrature detection into 1024 complex points for 730  $t_1$ -values, using the TPPI method.<sup>17,18</sup> For each  $t_1$ -value 64 transients were used with a delay of 2 s between each transient. During the recycle delay the water signal was suppressed with a weak irradiation pulse of 20 Hz. In all experiments a mixing time of 400 ms was used.

The data were processed with the program FELIX from Hare Research, Inc on a SGI-4D/25 computer. The one-dimensional FIDs were Fourier-transformed and baseline-corrected with a first-order polynomial fit. The water signal was set to 4.7 ppm, and the other signals were referenced to this signal. Line widths were measured directly from the spectra.

The 2D data were zero-filled to 2048 complex points along  $t_2$ , apodized with a 90° phase-shifted and squared sine-bell function, and multiplied with an exponential

function of 2 Hz. The spectra were baseline-corrected with a second-order polynomial fit. The FIDs along  $t_1$  were zero-filled to 4096 complex points and apodized with a 90° phase-shifted sine-bell function.

## Results and discussion

### *Spectra and assignment of proton resonances*

The spectral assignments of oligomers **I** and **II** have previously been reported by Gronenborn *et al.*<sup>15</sup> and by Frey and Leupin,<sup>16</sup> respectively. These assignments have been checked by 2D COSY and NOESY experiments and the agreement is satisfactory taking into account the difference in recording temperature. A sequential walk in the H2/H6/H8–H1'-region is indicated for sequences **I** and **II** in Figs 4 and 5, respectively. The duplexes are associated in solution end-on, producing a strong NOE cross-peak between C1–H1' and G6–H8.

In regular B-type DNA three A–H2···H1' cross-peaks are usually observed: intra-nucleotide, intra-strand and cross-strand A–H2( $n$ )···H1' ( $m + 1$ ) ( $n$  and  $m$  are complementary residues). These distances are usually found in the range 3.5–5 Å, depending on sequence-dependent variations.<sup>19</sup> In **I** the intra-nucleotide peak and the cross-strand peak overlap due to symmetry. However, the presence of an unusual NOE peak corresponding to a A–H2···G6–H1' dipolar interaction is difficult to rationalize in terms of regular B-DNA geometry. Since the A–H2 proton has relatively long  $T_1$ -relaxation time in a hexamer, the peak may be explained as artifact due to severe  $t_1$ -noise. Gronenborn *et al.*<sup>15</sup> have used 1D NOE data to determine the 3D solution structure of **I** and arrive at a conventional B-type structure. This result corresponds, qualitatively, with our 2D data. In particular, the aromatic-aromatic region in which all the inter-base H6/8( $n$ )···H6/8( $n + 1$ ) NOE peaks are observed (data not shown) confirms the presence of a stacked structure that also includes the terminal residues.

In **II** an unusually large intra-strand A–H2···TH1' cross-peak is observed while the expected cross-strand A–H2···GH1' peak is missing. Nilges *et al.*<sup>20</sup> have carried out a structure determination of **II** by a combination of 2D NOESY intensities and restrained molecular dynamics calculations. In the latter case the structure is found to be of the B-type and exhibits clear sequence-dependent variations in helical parameters. In addition, the structure appears to be bent at the Pyr–Pur step with a radius of approximately 20 Å. Recently, Metzler *et al.*<sup>21</sup> and Chuprina *et al.*<sup>19</sup> have claimed that global helical parameters (e.g. degree of bending) determined by NMR and molecular dynamics calculations have rather low accuracy.

The linewidths of the proton signals are seen to be markedly different for the two sequences (Figs. 1 and 2). GCATGC have relatively broad lines while the inverted sequence CGTACG have quite narrow lines. In the latter case this might imply a single helix structure; however,

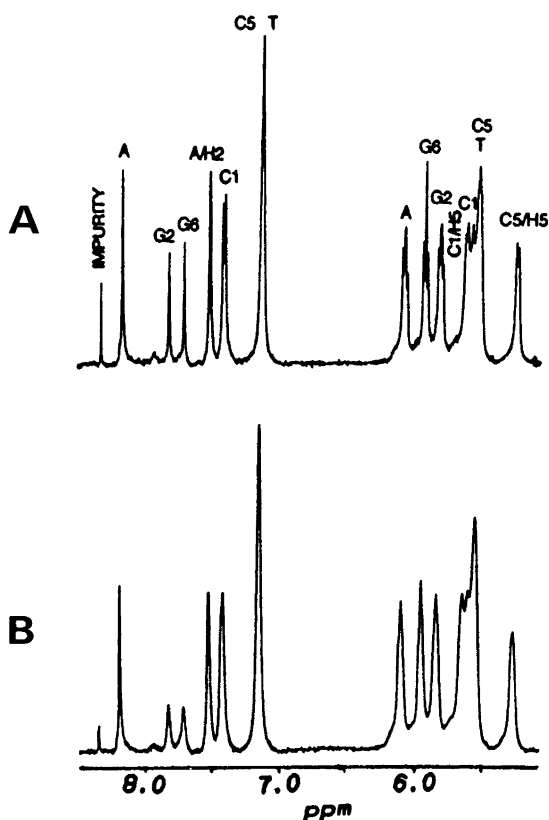


Fig. 1. 400 MHz  $^1\text{H}$  NMR spectra of the aromatic and anomeric region of the hexamer 5'-d(CG TACG) $_2$  comprising the specific target site for the restriction endonuclease *Sph* I. The temperature was 303 K. Concentration of  $\text{MnCl}_2$ : (A) 0 and (B) 0.3 mM.

the imino signals (not shown) confirm the presence of a double helical structure. Also the complete stacking pattern revealed in the aromatic-aromatic region indicates the presence of a regular helix. The differences in linewidths may be related to inherent helix stability of the two sequences. Simple theoretical calculations of total helical stacking energy<sup>22</sup> give  $-48.9 \text{ kcal mol}^{-1}$  dimer and  $-44.3 \text{ kcal mol}^{-1}$  dimer for **I** and **II**, respectively.

**1D Mn(II) titration.** The successive additions of Mn(II) ions to samples of d(CG TACG) $_2$  and d(GCATGC) $_2$  produce selective line-broadening of proton resonances as shown in Figs. 1 and 2. The guanine H8 protons show the most dramatic effects, while the non-G residues show almost no selective line-broadening. In the first part of the titrations 0.15 mM EDTA was saturated. A fraction of the EDTA added is complexed to the ubiquitous traces of paramagnetic impurities in the samples. A large paramagnetic effect is experienced by the terminal 5'-G1-H8 signal in GCATGC, while the effect on G5-H8 is negligible. In CGTACG the H8 signals on G2 and G6 exhibit almost the same degree of paramagnetic induced broadening as G1 in **II**. The qualitative order of paramagnetic

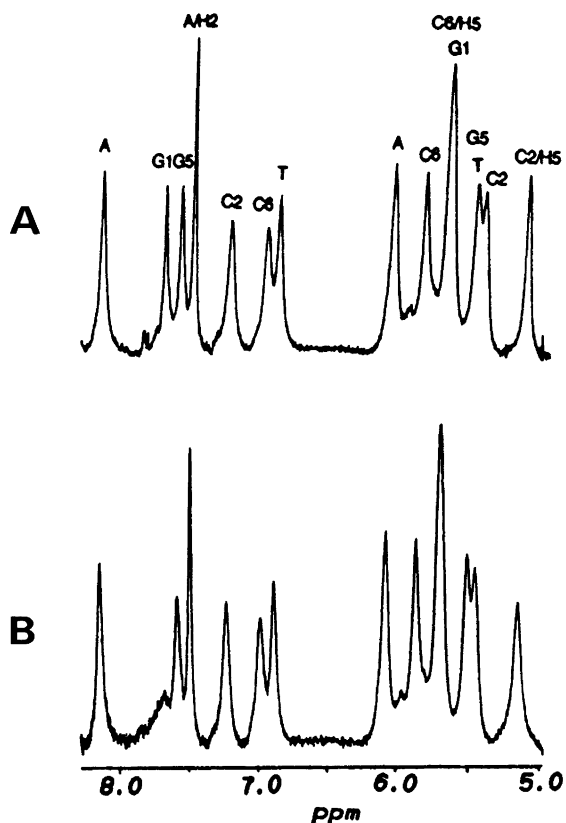


Fig. 2. 400 MHz  $^1\text{H}$  NMR spectra of the aromatic and anomeric region of the hexamer 5'-d(GCATGC) $_2$  titrated with  $\text{MnCl}_2$ . Concentration of  $\text{MnCl}_2$ : (A) 0 and (B) 0.7 mM.

influence on the purine H8 resonances is, 5'-G1 = G2 = G6 > G5.

The selective, paramagnetic line-broadening of H8 resonance is most easily explained by an interaction between  $\text{Mn}^{2+}$  and nitrogen G-N7. We do not know in advance which relaxation mechanism dominates the paramagnetic contribution to the linewidth in each

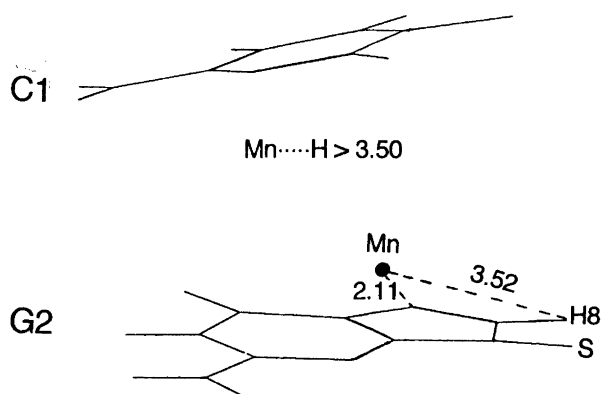


Fig. 3. A possible binding mode of  $\text{Mn}^{2+}$  to the guanine residue. The orientation of the CG bases are based on the solution structure of a dodecamer sequence as determined from 2D NMR data.<sup>23</sup>

specific case. If, for instance, a G-N7...Mn bond is established, the relaxation of H8 is most certainly dominated by scalar paramagnetic relaxation. If there is not a direct bond, the line-broadening effect is probably due to dipolar paramagnetic relaxation (through-space). Such an arrangement is possible if  $Mn^{2+}$  interacts mainly with the phosphate group 5'-C-p-G-3'. Crystal structures of transition-metal ion - mononucleotide complexes strongly support the supposition that N7 is the binding site in solution. In the oligomer the N7 site is exposed and easily assessable for attack from metal ions. In Fig. 3 the orientation of the first two bases in the dodecamer 5'-d(CGCGAATTCGCG)<sub>2</sub> is shown as determined from NMR data.<sup>23</sup> The position of the probable binding site for  $Mn^{2+}$  is indicated. A second possible binding mode is formation of a chelate between N7 and O6 on guanine. However, even though theoretical calculations have shown this mode to be favorable,<sup>24</sup> it has never been observed for complexes of guanine.

**2D Mn(II) titration.** Figures 4 and 5 show the NOESY maps of the H8/H6-H1 region of sequences I and II, respectively, with and without  $MnCl_2$ . A complete sequential walk is indicated for the unperturbed system (Figs. 4A and 5A). Addition of  $MnCl_2$  is shown to quench effectively the dipolar NOE interaction for the protons close to the binding sites of paramagnetic ions (Figs. 4B and 5B). In sequence I the inter-residue G2-H8...C1-H1' and G6-H8...T3-H1' cross-peaks are eliminated, while the corresponding base-sugar intra-residue peaks are appreciably reduced in intensity. In the NOESY map of II based on a sample with higher Mn concentration both the inter-residue and intra-residue cross-peaks involving G1-H8...H1' interaction are absent. The dramatic effects on NOESY intensities produced by paramagnetic ions clearly demonstrate how paramagnetic impurities can lead to large errors in structure determinations based on 2D NMR intensity data.

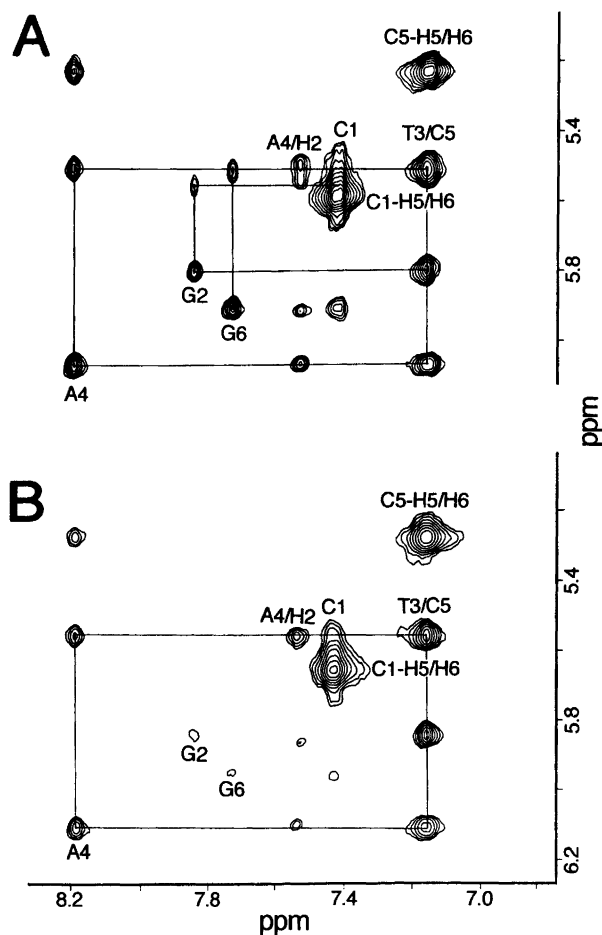


Fig. 4. Contour plots of the H8/H6-H1'/H5 region in the 400 MHz NOESY spectra of the 5'-d(CGATCG)<sub>2</sub> hexamer (400 ms mixing time). The intra-residue H8/H6-H1' cross-peaks are labeled with the residue number. The sequential connectivity is indicated with a solid line. (A) Without  $MnCl_2$ ; (B) with 0.10 mM  $MnCl_2$ .

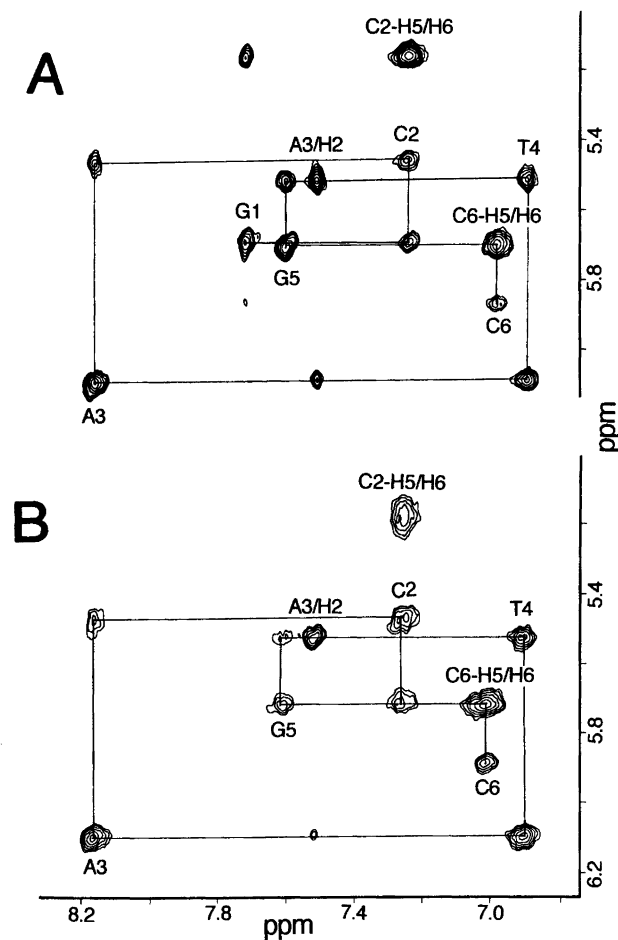


Fig. 5. Contour plots of the H8/H6-H1'/H5 region in the 400 MHz NOESY spectra of the 5'-(GCATGC)<sub>2</sub> hexamer (400 ms mixing time). (A) Without  $MnCl_2$ ; (B) with 0.99 mM  $MnCl_2$ .

*Rules for selective metal binding.* Based on our earlier studies on Mn(II) ion-oligonucleotide interactions<sup>8</sup> we suggested the following rule for selective metal binding to G-residues on the 5'-side: 5'-GG = GA > GT ≫ GC. The selectivity was explained, qualitatively, by sequence-dependent variation in molecular electrostatic potentials (MEP) along the oligonucleotide chain.<sup>10</sup> The sequences included in the present study contain GC and GT but no GG or GA base steps. The dramatic effect on the terminal 5'-G1 in GCATGC has not been observed in previously studied oligonucleotides (dodecamers) in which the starting base step was 5'-GC.<sup>8</sup> The degree of 'fraying' at the terminal bases may be different for hexamers and dodecamers, leaving the potential binding sites more or less exposed to metal ions. Except for differences in end-effects we may also have to invoke a three-base context to explain the observed affinity in those cases where there are no high-affinity G-purine steps present. The 5'-GC sequences studied earlier showing no G1 interaction had terminal 5'-GCC-steps as compared to a 5'-GCA-step in II. In order to check the hypothesis of a three-base pair context to account for metal ion selectivity a large variety of sequences will have to be tested.

A comparison of the G-affinity between GCATGC and CGTACG reveals a selectivity pattern for the central guanines in agreement with the suggested rule (G2-T3 > G5-C6). Both steric and electrostatic factors govern metal coordination; e.g. the manganese binding pattern is completely different from that observed for mercury.<sup>9</sup> Hg(II) ions are found to prefer thymines in 5'-d(CGCGAATTCGCG)<sub>2</sub>, producing a 'bubble' on the double helix. The exact nature of the Hg...T interaction is not yet determined.

Both the donor strength of the ligating atoms and the preferred coordination geometry of the metal ions are important factors for determining metal ion-DNA selectivity. We are presently investigating the selectivity pattern for several transition metals. This work may be of importance in the search for better metal-based anti-tumor drugs which are assumed to interact selectively at the nucleic acid level. Several non-platinum metal complexes have shown promising anti-tumor activity and are presently being subjected to clinical trials.<sup>25</sup>

## References

1. Howell, S. B., Ed. *Platinum and Other Metal Coordination Compounds in Cancer Chemotherapy*, Plenum Press, New York 1991.
2. Fichtinger-Schepman, A. M., Van der Veer, J. L., den Hartog, J. H. J., Lohman, P. M. H. and Reedijk, J. *Biochemistry* 24 (1985) 707.
3. Braunlin, W. H., Drakenberg, T. and Nordenskiöld, L. *Biopolymers* 26 (1987) 1047.
4. Braunlin, W. H., Nordenskiöld, L. and Drakenberg, T. *Biopolymers* 28 (1989) 1339.
5. Rose, D. M., Polnaszek, C. F. and Bryant, R. G. *Biopolymers* 21 (1982) 653.
6. Frøystein, N. Å. and Sletten, E. *Acta Chem. Scand.* 45 (1991) 219.
7. Jia, X., Zon, G. and Marzilli, L. G. *Inorg. Chem.* 30 (1991) 228.
8. Frøystein, N. Å., Davis, J. T., Reid, B. R. and Sletten, E. *Acta Chem. Scand.* 47 (1993) 649.
9. Frøystein, N. Å. and Sletten, E., *J. Am. Chem. Soc.* 116 (1994). *In press.*
10. Pullman, A. and Pullman, B. *Q. Rev. Biophys.* 14 (1981) 289.
11. Wurdeman, R. L., Church, K. M. and Gold, B. *J. Am. Chem. Soc.* 111 (1989) 6408.
12. Kowalewski, J., Nordenskiöld, L. and Westlund, P. O. *Progr. NMR Spectrosc.* 17 (1985) 141.
13. Berger, N. A. and Eichhorn, G. L. *J. Am. Chem. Soc.* 93 (1971) 7062.
14. Hare, D. R., Wemmer, D. E., Chou, S. H., Drobny, G. and Reid, B. R. *J. Mol. Biol.* 171 (1983) 319.
15. Gronenborn, A. M., Clore, G. M. and Kimber, B. J. *Biochem. J.* 221 (1984) 723.
16. Frey, M. H. and Leupin, W. *Biopolymers* 24 (1985) 2371.
17. Redfield, A. G. and Kuntz, S. D. *J. Magn. Reson.* 19 (1975) 250.
18. Bodenhausen, G., Kogler, H. and Ernst, R. R. *J. Magn. Reson.* 58 (1984) 370.
19. Chuprina, V. P., Sletten, E. and Fedoroff, O. Y. *J. Biomol. Struct. Dyn.* 10 (1993) 693.
20. Nilges, M., Clore, G. M. and Gronenborn, A. M. *Biochemistry* 26 (1987) 3718.
21. Metzler, W. J., Wang, C., Kitchen, D. B., Levy, R. M. and Pardi, A. *J. Mol. Biol.* 214 (1990) 711.
22. Ornstein, R. L., Rein, R., Breen, D. L. and MacElroy, R. D. *Biopolymers* 17 (1978) 2341.
23. Nerdal, W., Hare, D. R. and Reid, B. R. *J. Mol. Biol.* 201 (1988) 717.
24. Perathia, D., Pullman, A. and Pullman, B. *Theor. Chim. Acta* 43 (1977) 207.
25. See Gielen, M. F., Ed. *Metal-Based Anti-Tumor Drugs*, Freund Publishing House, London 1988.

Received August 28, 1993.